

---

# *Array Imaging in Random Media Part II*

Chrysoula Tsogka

tsogka@tem.uoc.gr

University of Crete & FORTH-IACM

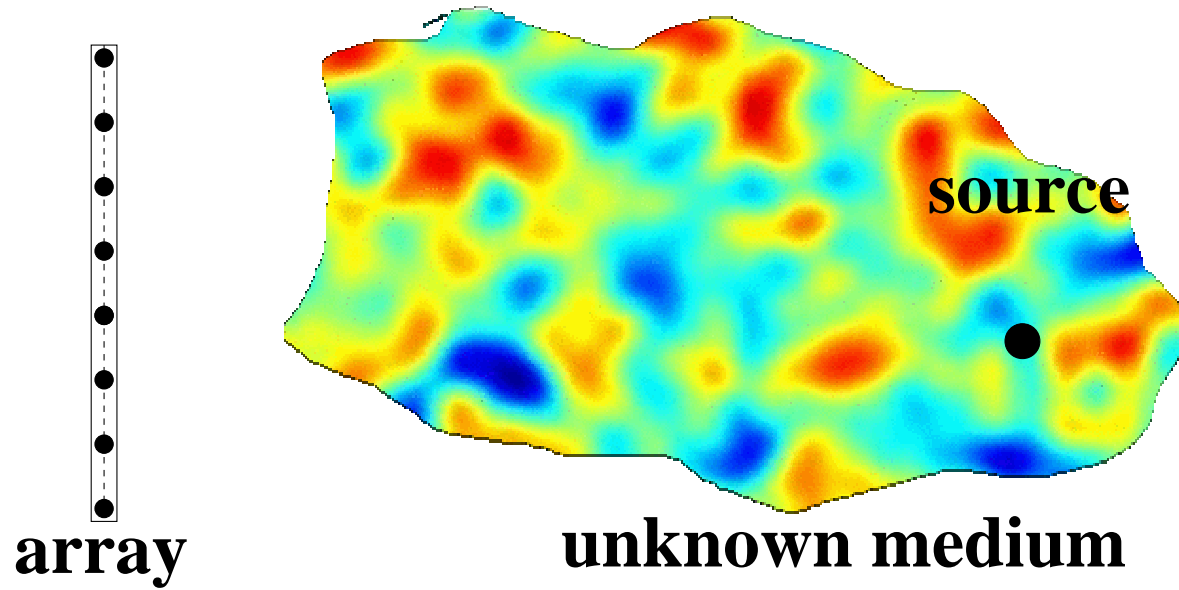
**In Collaboration with:**

Liliana Borcea (Rice University)

George Papanicolaou (Stanford University)

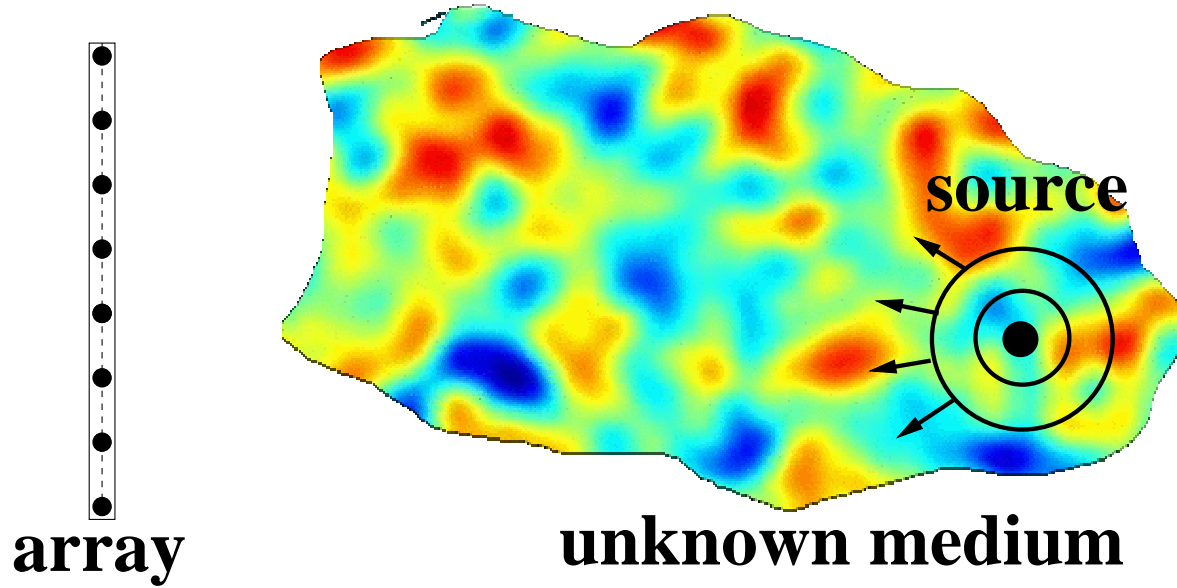
# The Time reversal process

---



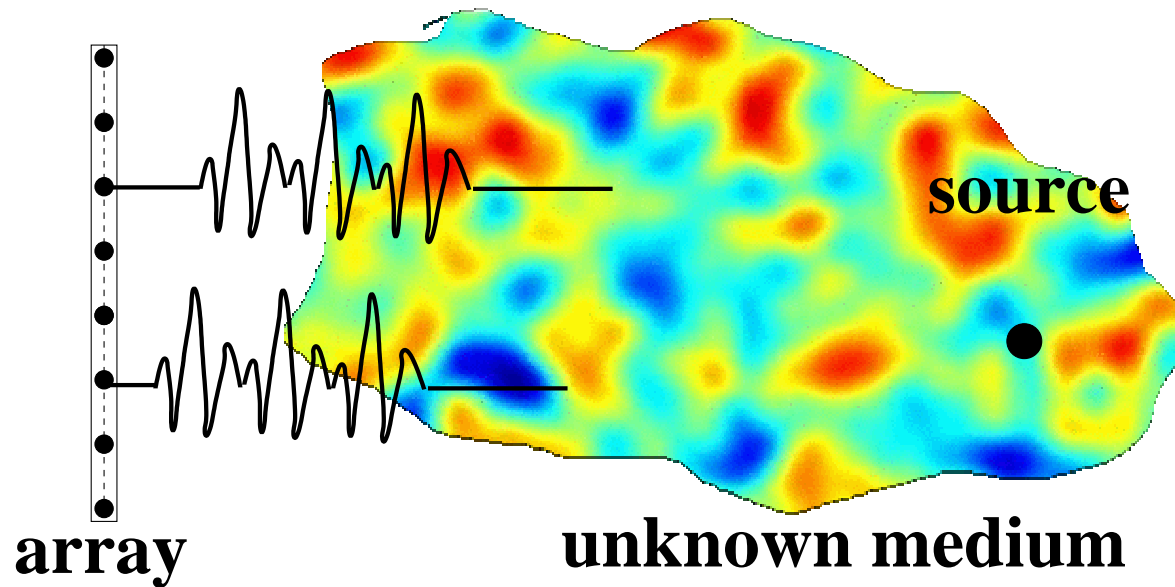
# The Time reversal process

---



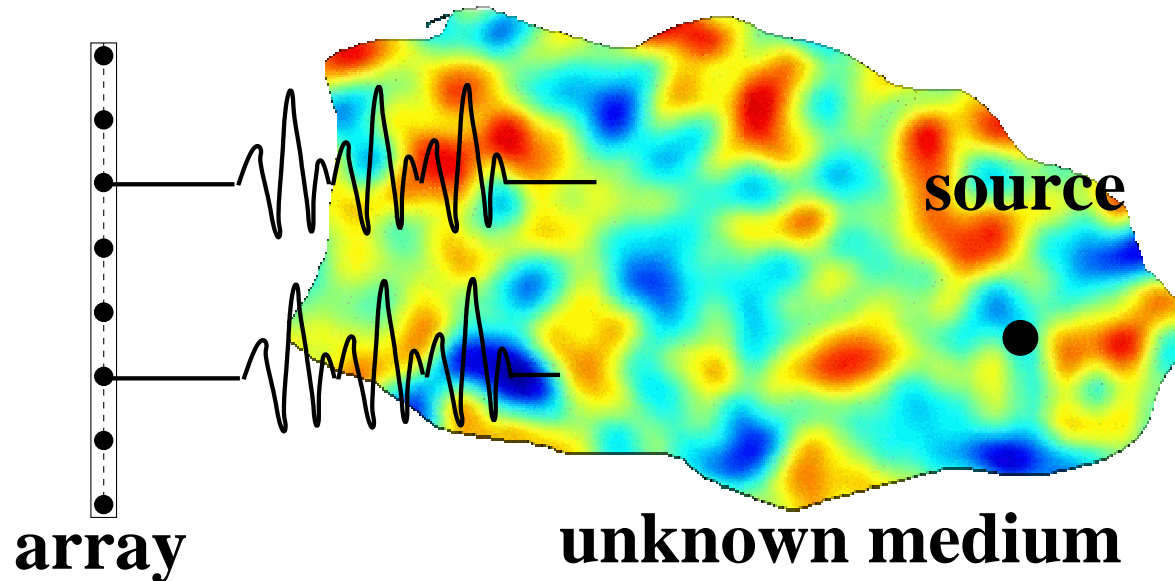
- The source sends a pulse

# The Time reversal process



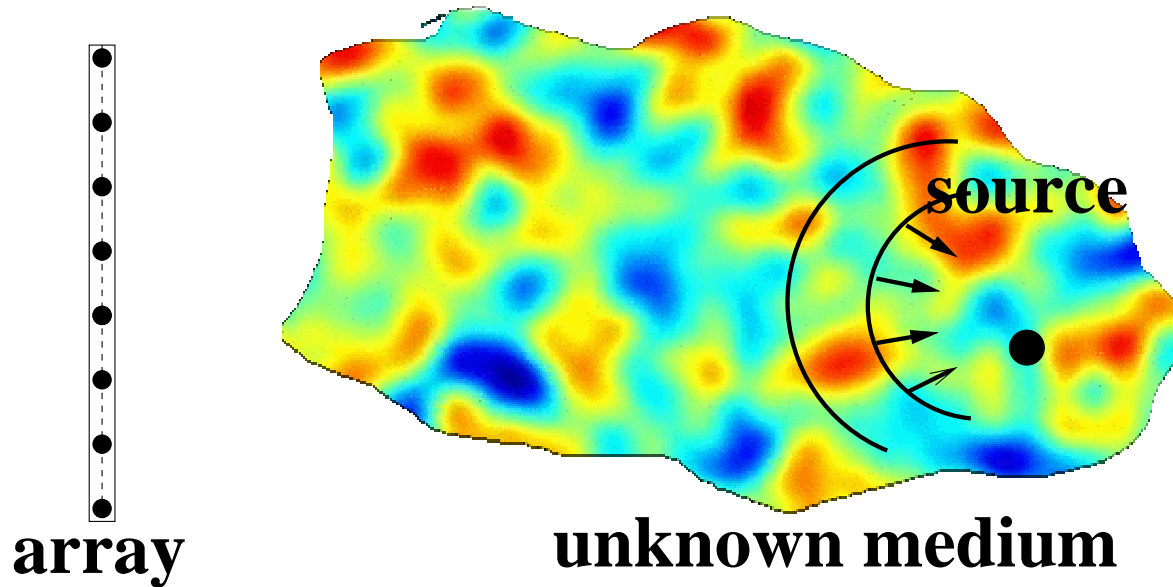
- The source sends a pulse
- The response is recorded at all array elements

# The Time reversal process



- The source sends a pulse
- The response is recorded at all array elements
- The recorded signals are time-reversed and re-emitted

# The Time reversal process



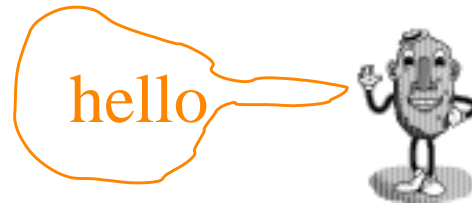
- The source sends a pulse
- The response is recorded at all array elements
- The recorded signals are time-reversed and re-emitted
- The wave focuses to the original source position

# Applications/Physical experiments

- M. Fink & al



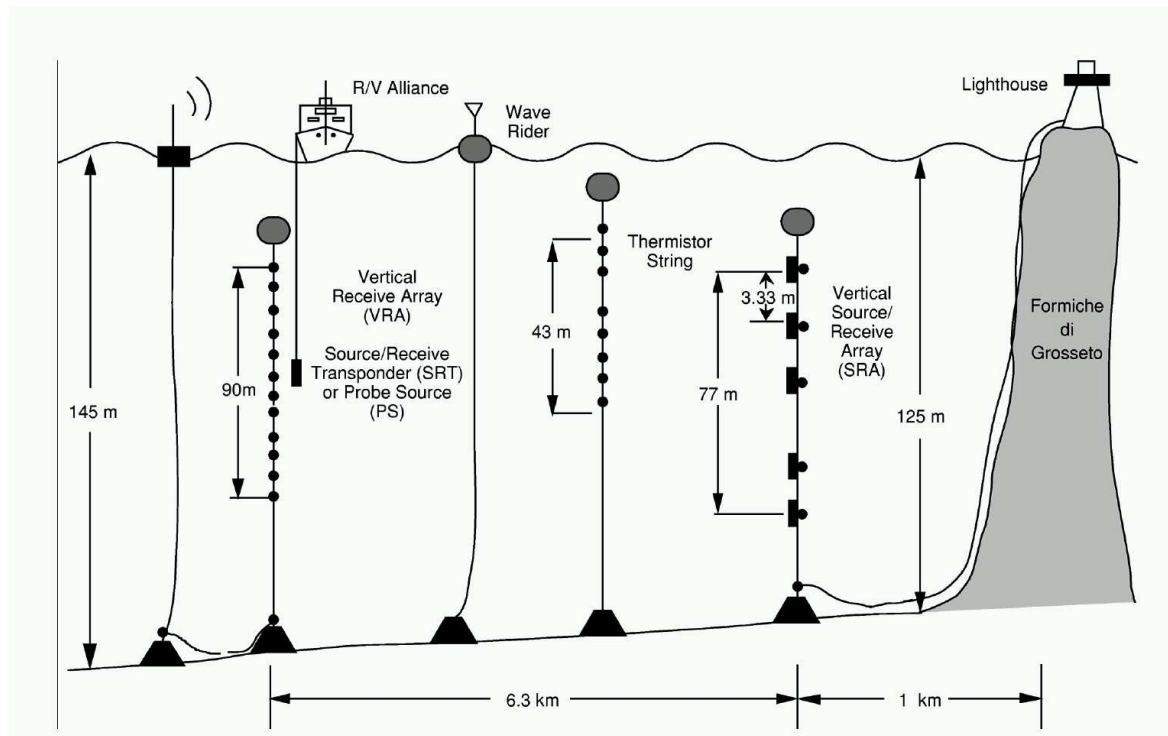
**array**



- IEEE Ultrasonics Symp. Proc., 1, pp. 681-686, Montreal, 1989.
- Time-reversed acoustics, Scientific American, 281, pp. 91-97, 1999.
- Time Reversal of Electromagnetic Waves, Phys. Rev. Letters, 92, 2004.

# Experiments: underwater acoustics

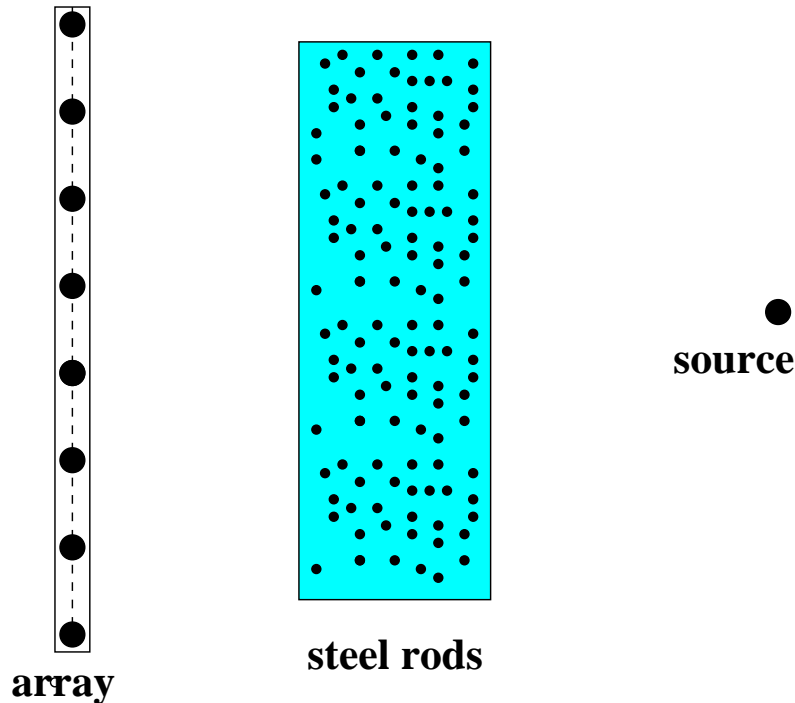
## ● W. A. Kuperman & al



- Phase conjugation in the ocean: Experimental demonstration of an acoustic time-reversal mirror, *JASA*, **103**, pp. 25-40, 1998.
- A long-range and variable focus phase-conjugation experiment in shallow water, *JASA*, **105**, pp. 1597-1604, 1999.
- Iterative time reversal in the ocean, *JASA*, **105**, pp. 3176-3184, 1999.

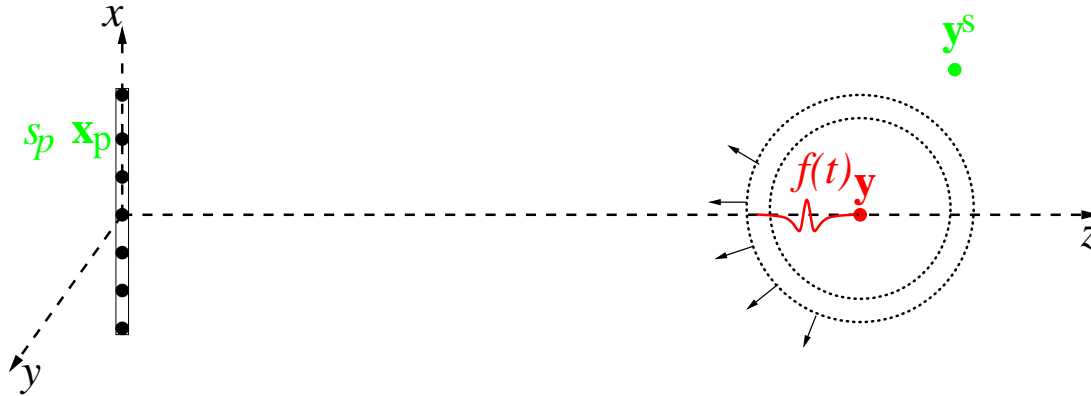
# Experiments: random media

## ● M. Fink & al



- Random multiple scattering of ultrasound. I. Coherent and ballistic waves, Phys. Rev. E, **64**, 2001.
- Random multiple scattering of ultrasound. II. Is time reversal a self-averaging process?, Phys. Rev. E, **64**, 2001.

# Time reversal : model

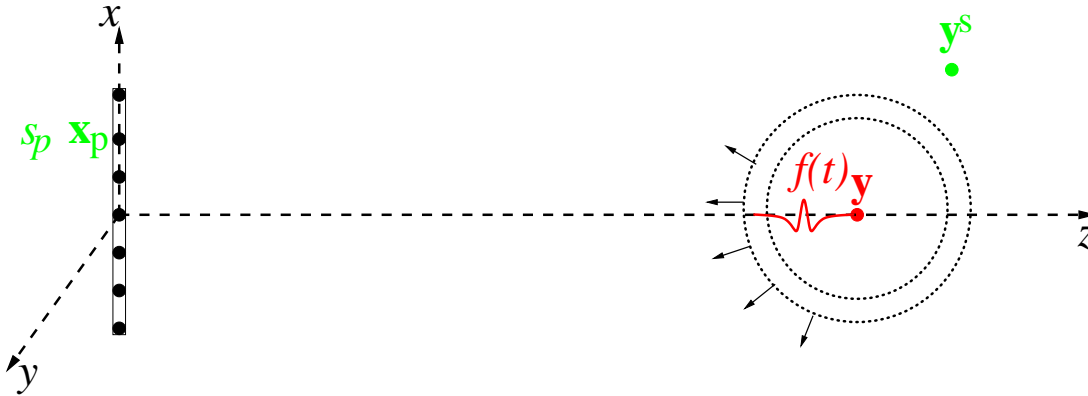


- point source located at  $\mathbf{y} = (0, 0, L)$  sends pulse  $f(t)$
- array element  $\mathbf{x}_p = (x_p, 0, 0)$  receives  $s_p$ ,

$$s_p = f(t) * G(\mathbf{x}_p, \mathbf{y}, t) = \frac{1}{2\pi} \int_{-\infty}^{\infty} \hat{f}(\omega) \hat{G}(\mathbf{x}_p, \mathbf{y}, \omega) d\omega$$

$$\hat{s}_p(\omega) = \hat{f}(\omega) \hat{G}(\mathbf{x}_p, \mathbf{y}, \omega)$$

# Time reversal : model



- the signals  $s_p$  are time reversed and re-emitted into the **real** medium
- the field at search point  $\mathbf{y}^S = (\xi^S, z^S)$  is

$$\hat{\Gamma}^{\text{TR}}(\mathbf{y}^S, \omega) = \overline{\hat{f}(\omega)} \sum_p \overline{\hat{G}(\mathbf{x}_p, \mathbf{y}, \omega)} \hat{G}(\mathbf{x}_p, \mathbf{y}^S, \omega)$$

# Time reversal in random media

---

- Fundamental properties

statistical stability & super-resolution

# Time reversal in random media

---

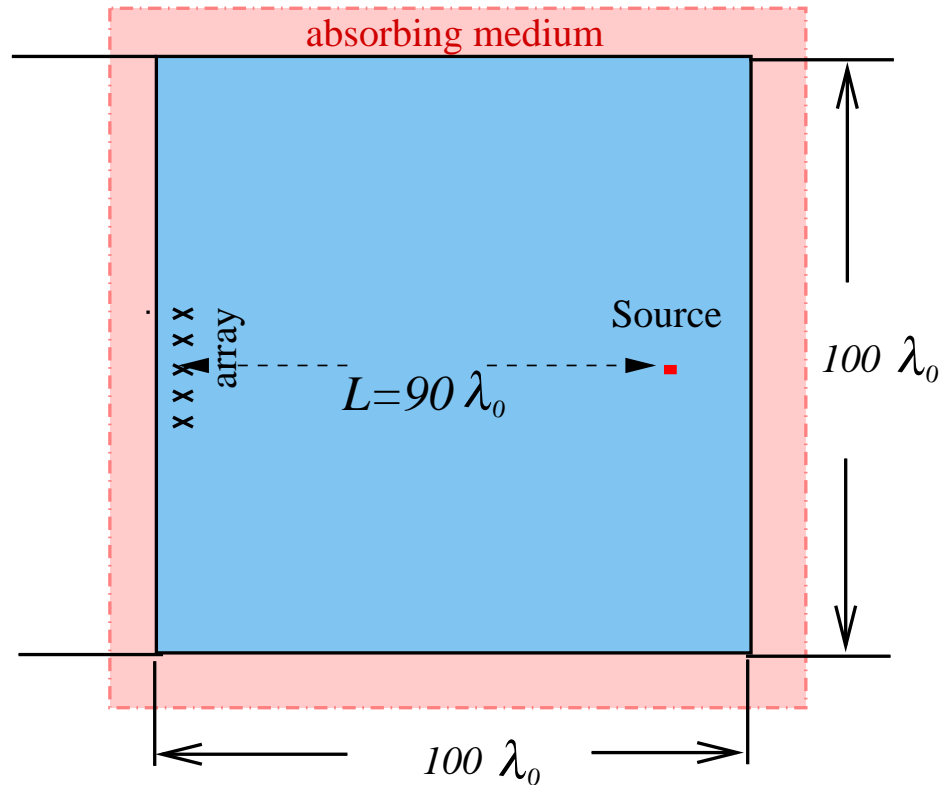
- Fundamental properties
  - **statistical stability & super-resolution**
- Theoretical studies (and references there in)
  - J.F Clouet, J.P Fouque, *A time reversal method for an acoustical pulse propagating in randomly layered media*, *Wave Motion*, **25**, pp. 361-168, 1997.
  - P. Blomgren, G. Papanicolaou, H. Zhao, *Super-Resolution in Time-Reversal Acoustics*, *JASA*, **111**, pp. 238-248, 2002.
  - G. Bal, G. Papanicolaou, L. Ryzhic, *Self averaging in time-reversal for the parabolic wave equation*, *Stoch. Dyn.*, **2**, pp. 507-531, 2002.
  - G. Papanicolaou, L. Ryzhic, K. Solna, *Statistical stability in time reversal*, *SIAM J. Appl. Math.*, **64**, pp. 1133-1155, 2004.

# Time reversal in random media

---

- Fundamental properties
  - statistical stability & super-resolution
- The regime (scaling)
  - remote sensing:  $a \ll L$
  - weak fluctuations:  $\sigma \leq 5\%$
  - important multipathing:  $\lambda_0 \sim \ell \ll a$
  - broad-band is essential !
  - L. Borcea, G. Papanicolaou, C. Tsogka, *Theory and applications of time reversal and interferometric imaging*, Inverse Problems, Vol 19, pp. S139-S164, 2003.

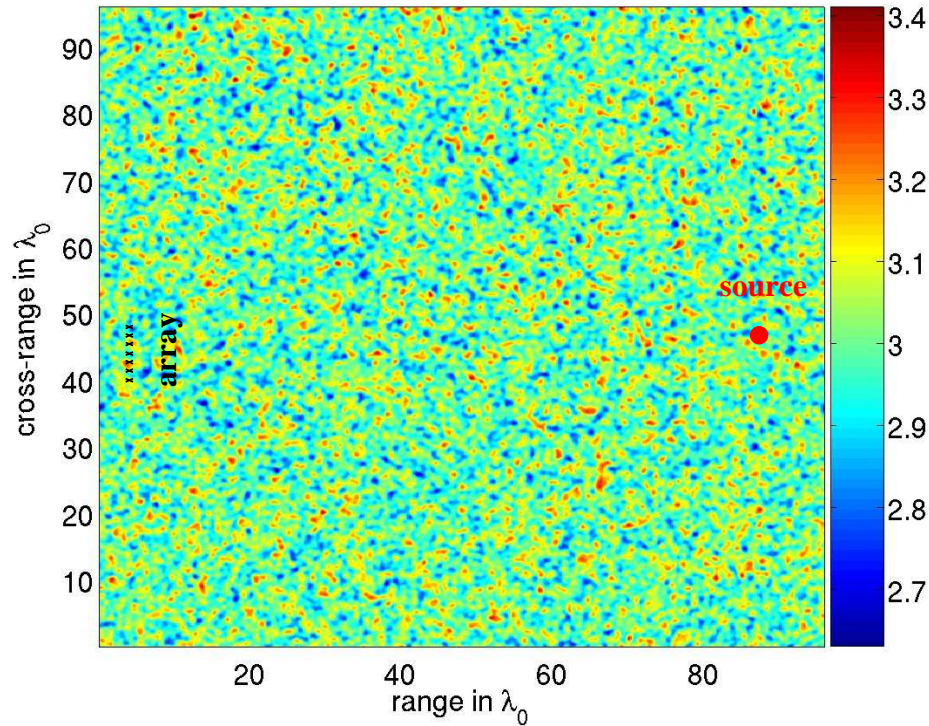
# Setup for the numerical simulations



In the context of ultrasound non-destructive testing

- Frequency range 150 – 450KHz,  $c_0 = 3\text{Km/s}$ ,  $\lambda_0 = 1\text{cm}$ .
- Linear array with  $N = 11$  elements of aperture  $a = 5\lambda_0$ . The range is  $L = 90\lambda_0$ . The source is a point.

# Setup for the numerical simulations



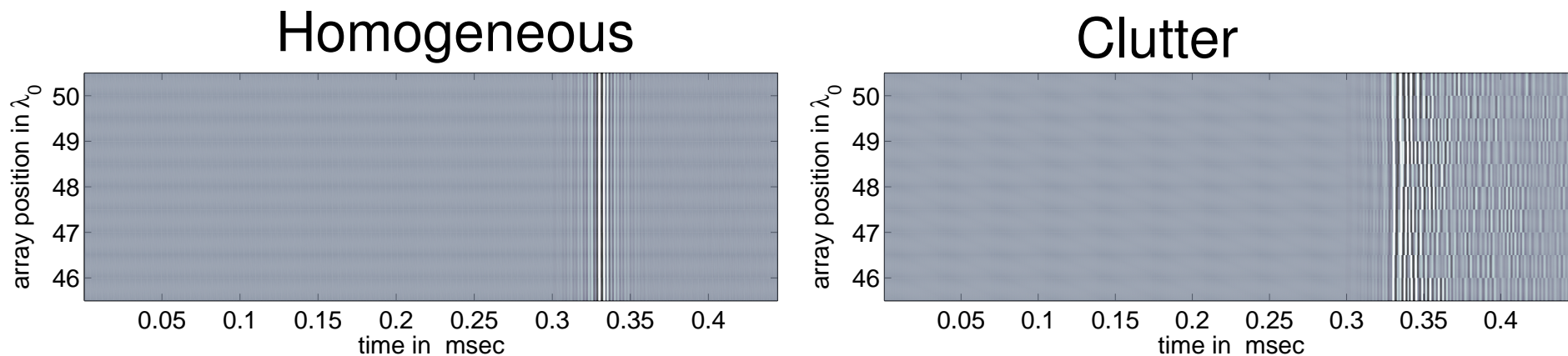
For the clutter:

- $\mu$  has a Gaussian correlation function

$$R(\mathbf{x}, \mathbf{x}') = \langle \mu(\mathbf{x})\mu(\mathbf{x}') \rangle = R(|\mathbf{x} - \mathbf{x}'|) = e^{-\frac{|\mathbf{x} - \mathbf{x}'|^2}{2\ell^2}}$$

- with  $\ell = 0.5\lambda_0$  and  $\sigma = 0.03$

# Data on the array: traces



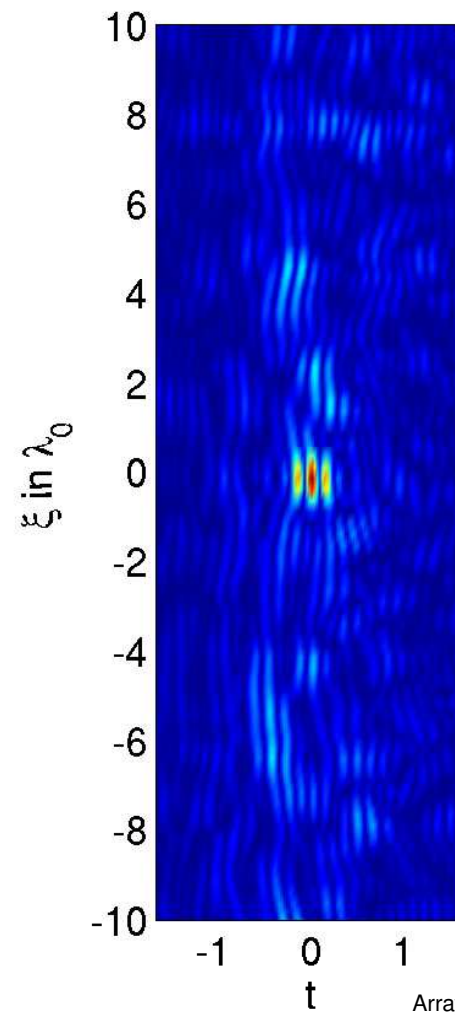
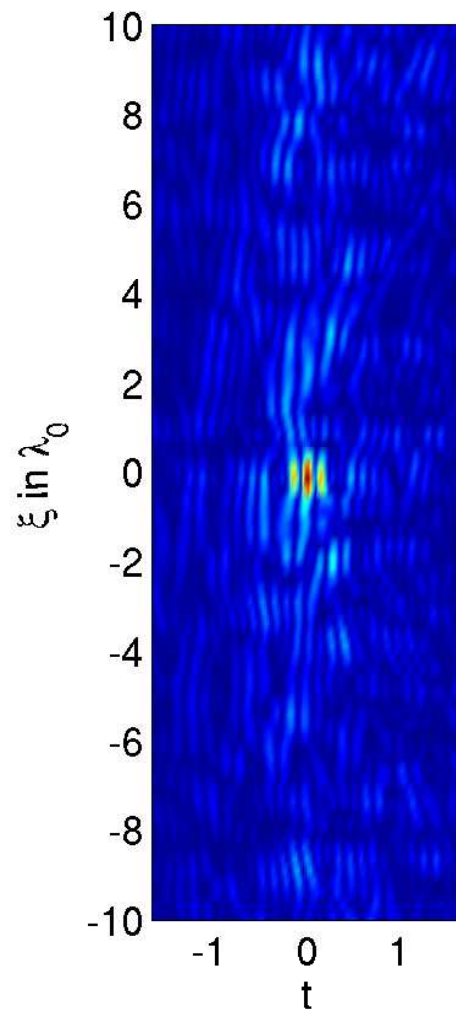
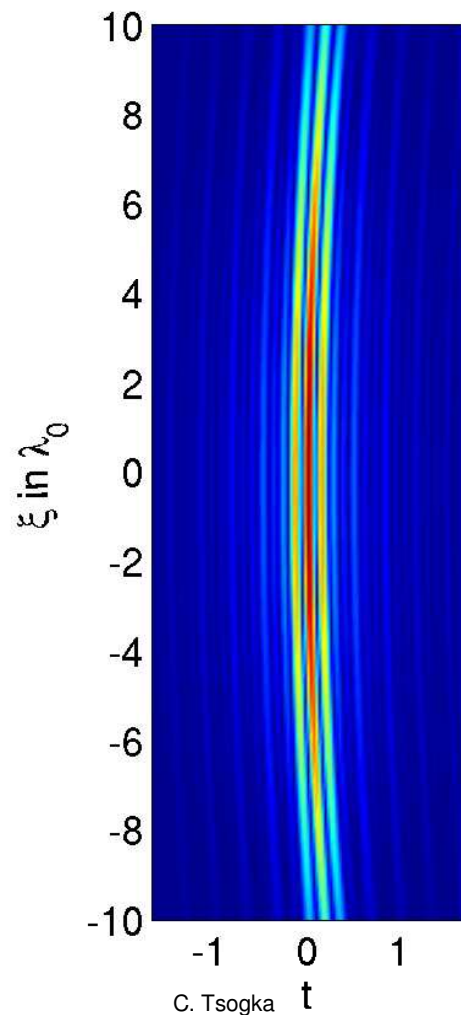
The clutter “helps” the time-reversal process as the significant multipathing of the waves by the inhomogeneities results to an array with a larger **effective** aperture!

# Time reversal results

$$\Gamma^{TR}(\mathbf{y}^S, t) \text{ at } \mathbf{y}^S = (\xi, z^S = L)$$

Homogeneous

Clutter (2 realizations)



# Time reversal: resolution analysis

- To estimate the spatial resolution in cross-range, let us evaluate  $\Gamma^{TR}$  at the exact range  $z^S = L$  and at the correct arrival time  $t_0$ .
- In **homogeneous** media we get

$$\Gamma_0^{TR}(\xi, L; t_0) \approx C \operatorname{sinc}\left(\frac{\pi\xi a}{\lambda_0 L}\right) e^{-\frac{\xi^2}{2\sigma_0^2}}$$

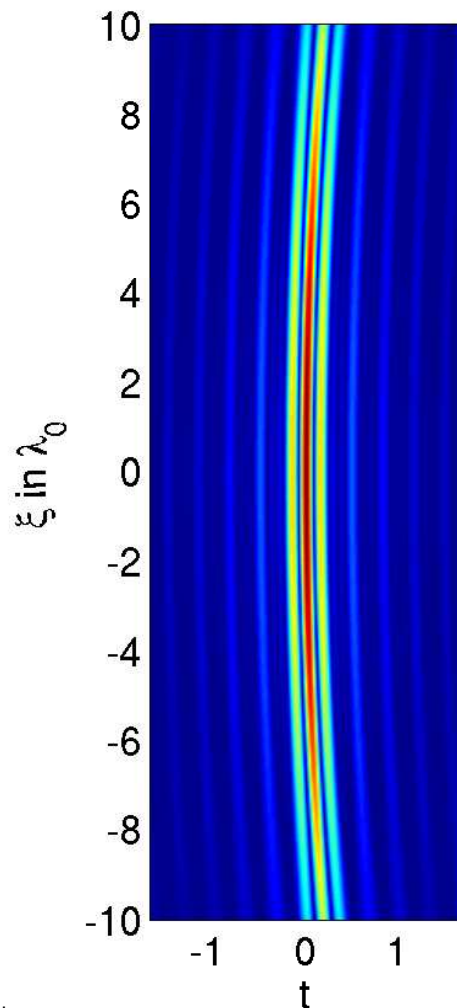
with  $\sigma_0 = \frac{2\lambda_0 L}{Ba}$

- narrow-band: sinc function  $\frac{\lambda_0 L}{a}$  + Fresnel zones
- broad-band: gaussian  $\sim \frac{\lambda_0 L}{a}$  no Fresnel zones

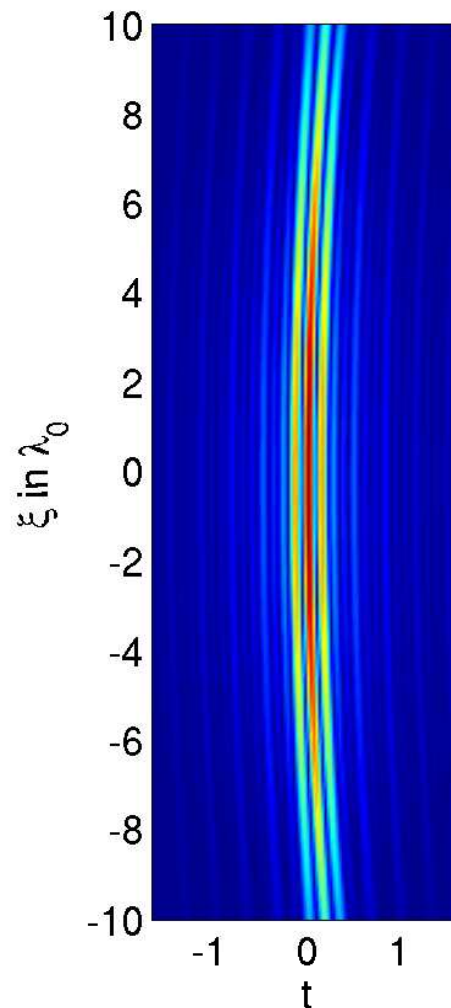
# TR focusing in homogeneous media

$$\Gamma_0^{\text{TR}}(\xi, L; t), t \times \xi : [-2, 2] \text{ms} \times \xi \in [-10, 10] \lambda_0$$

Theory



Numerics



# Time reversal: resolution analysis

- To estimate the spatial resolution in cross-range, let us evaluate  $\Gamma^{TR}$  at the exact range  $z^S = L$  and at the correct arrival time  $t_0$ .
- In **random** media we get

$$\Gamma_R^{TR}(\xi, L; t_0) \approx C e^{-\frac{\xi^2}{2\sigma_R^2}}$$

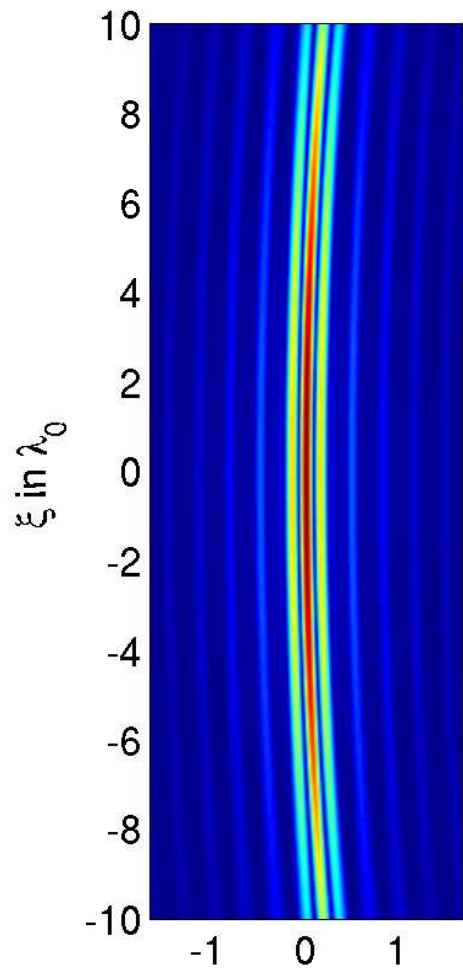
with  $\sigma_R = \frac{\lambda_0 L}{2\pi a_e}$

- the focal spot size becomes  $\sim \frac{\lambda_0 L}{a_e}$  instead of  $\sim \frac{\lambda_0 L}{a}$
- $a_e$ : effective array aperture ( $= \sqrt{DL^3}$ )

# TR focusing in random media

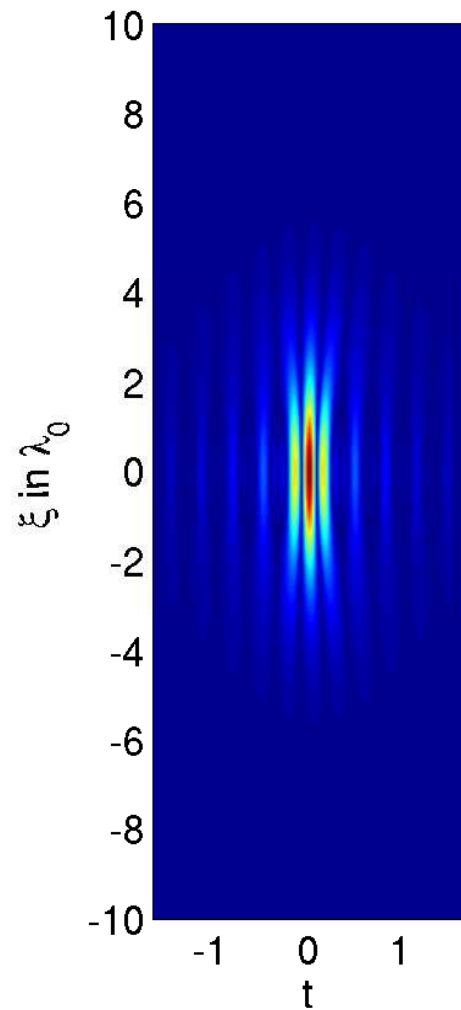
$$\Gamma_R^{\text{TR}}(\xi, L; t), t \times \xi : [-2, 2] \text{ms} \times \xi \in [-10, 10] \lambda_0$$

Homogeneous

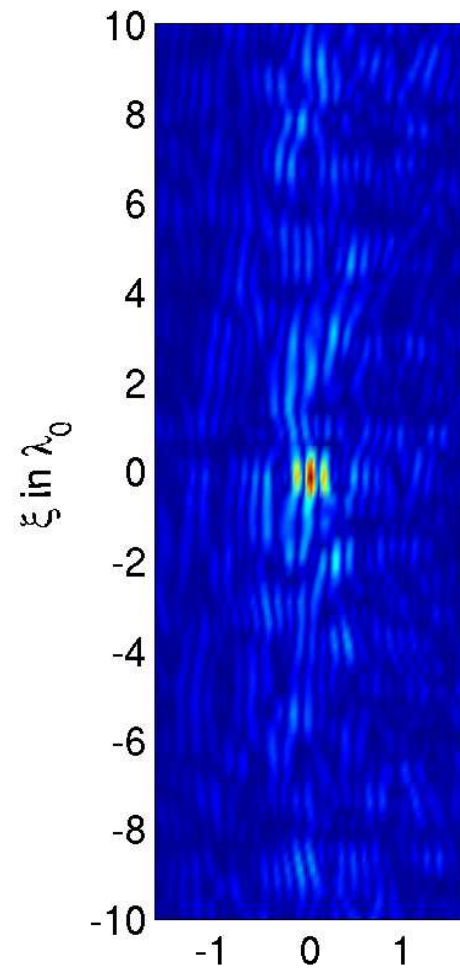


C. Tsogka

Random: Theory



Numerics

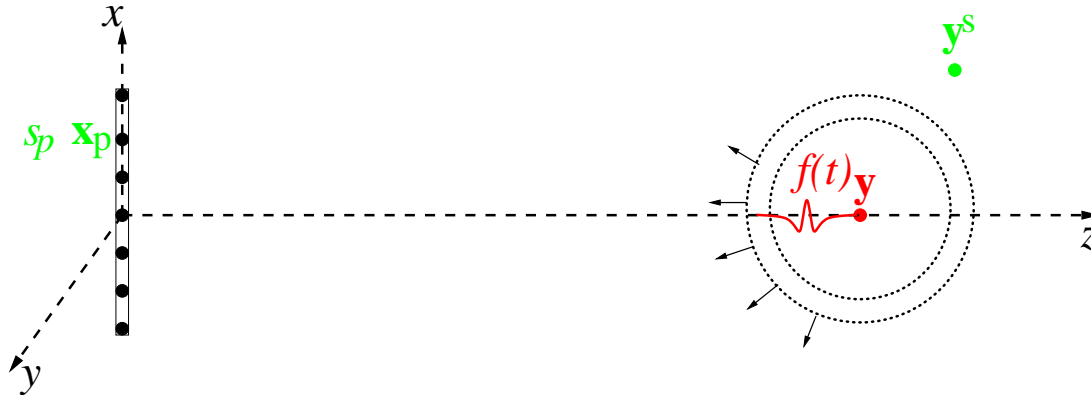


# Effective aperture estimation

---

- It is important in applications (wireless, sonar, etc) to know the size of the focal spot or equivalently the effective aperture.
- One way to do this, is experimentally by measuring the size of the focal spot (not feasible in practice).
- We propose to estimate  $a_e$  using an imaging method (MF or CINT).

# Matched Field Imaging (MF)

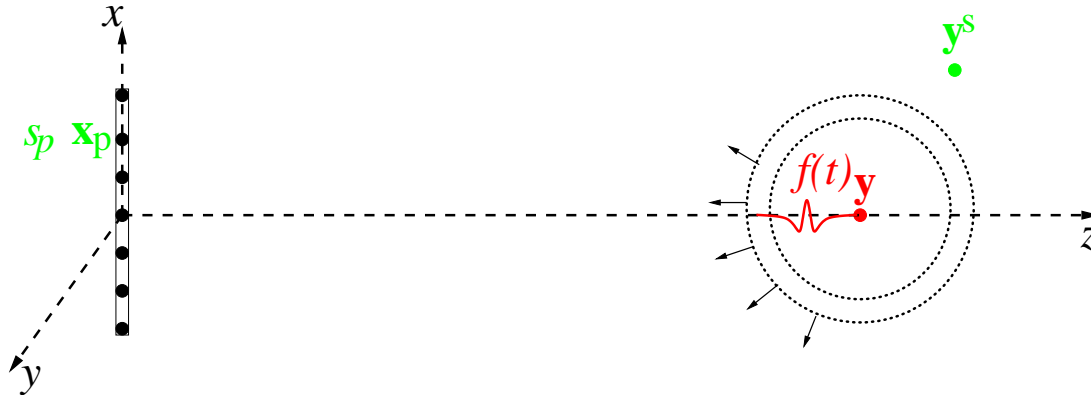


- point source located at  $\mathbf{y}$  sends pulse  $f(t)$
- array element  $\mathbf{x}_p$  receives  $s_p$ ,

$$\hat{s}_p(\omega) = \hat{f}(\omega) \hat{G}(\mathbf{x}_p, \mathbf{y}, \omega)$$

- the signals  $s_p$  time reversed and re-emitted into a **fictitious** medium

# Matched Field Imaging (MF)



- the field at search point  $\mathbf{y}^S$  is

$$\hat{\Gamma}^{IM}(\mathbf{y}^S, \omega) = \overline{\hat{f}(\omega)} \sum_p \overline{\hat{G}(\mathbf{x}_p, \mathbf{y}, \omega)} \hat{G}_0(\mathbf{x}_p, \mathbf{y}^S, \omega)$$

- to image we use the matched field method (MF):

$$\Gamma^{MF}(\mathbf{y}^S) = \int d\omega \left| \hat{\Gamma}^{IM}(\mathbf{y}^S, \omega) \right|^2$$

# Matched Field vs Time reversal

---

- Time reversal

$$\Gamma_R^{\text{TR}}(\xi, L; t_0) \approx C e^{-\frac{\xi^2 a_e^2 2\pi^2}{\lambda_0^2 L^2}}$$

- $a_e$  unknown parameter that depends on the statistics of the random medium

# Matched Field vs Time reversal

---

- Time reversal

$$\Gamma_R^{\text{TR}}(\xi, L; t_0) \approx C e^{-\frac{\xi^2 a_e^2 2\pi^2}{\lambda_0^2 L^2}}$$

- $a_e$  unknown parameter that depends on the statistics of the random medium
- Matched Field

$$\Gamma^{\text{MF}}(\xi, L + \eta) \approx C e^{-\frac{\xi^2}{2(L+\eta)^2} \left(\frac{L}{a_e}\right)^2}$$

# Matched Field vs Time reversal

- Time reversal

$$\Gamma_R^{\text{TR}}(\xi, L; t_0) \approx C e^{-\frac{\xi^2 a_e^2 2\pi^2}{\lambda_0^2 L^2}}$$

- $a_e$  unknown parameter that depends on the statistics of the random medium
- Matched Field

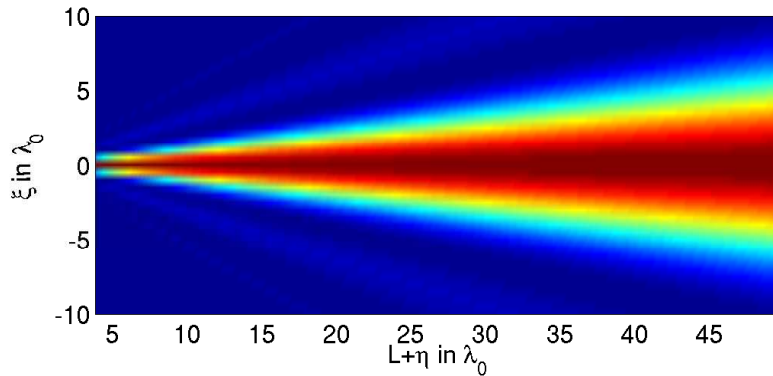
$$\Gamma^{\text{MF}}(\xi, L + \eta) \approx C e^{-\frac{\xi^2}{2(L+\eta)^2} \left(\frac{L}{a_e}\right)^2}$$

- Estimate  $a_e$  by matching **it** to the numer. comp. field  
(**need L**  $\Rightarrow$  get it from arrival times)

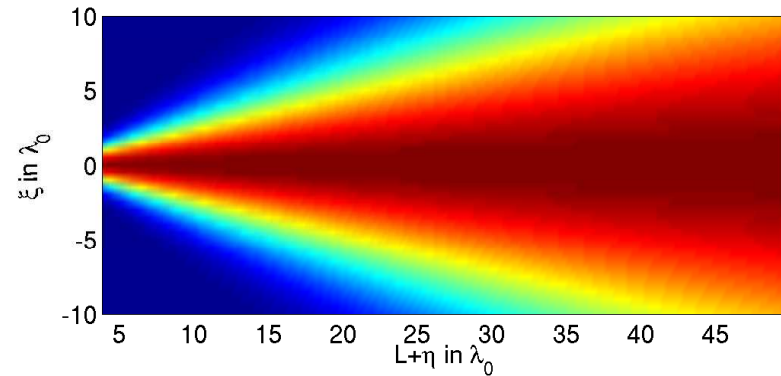
# Matched Field vs Time reversal

- Matched Field: resolution loss

homogeneous



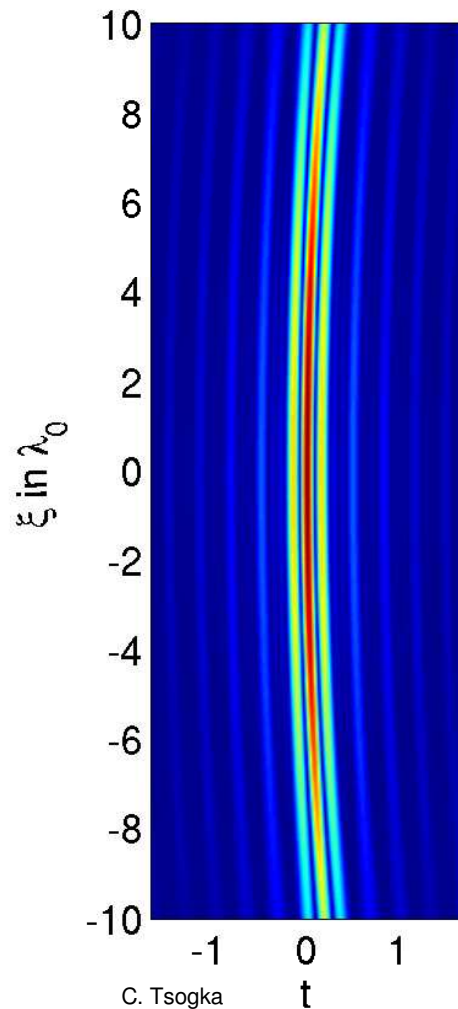
random



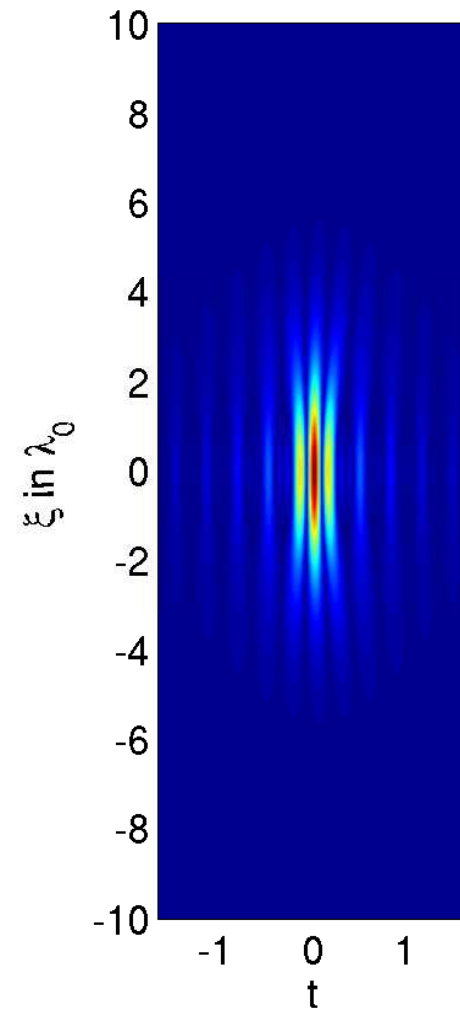
# Matched Field vs Time reversal

- Time Reversal: **super-resolution**

homogeneous



random



# Matched Field vs Time reversal

---

- Using the MF estimator for three realizations of the random medium we obtain

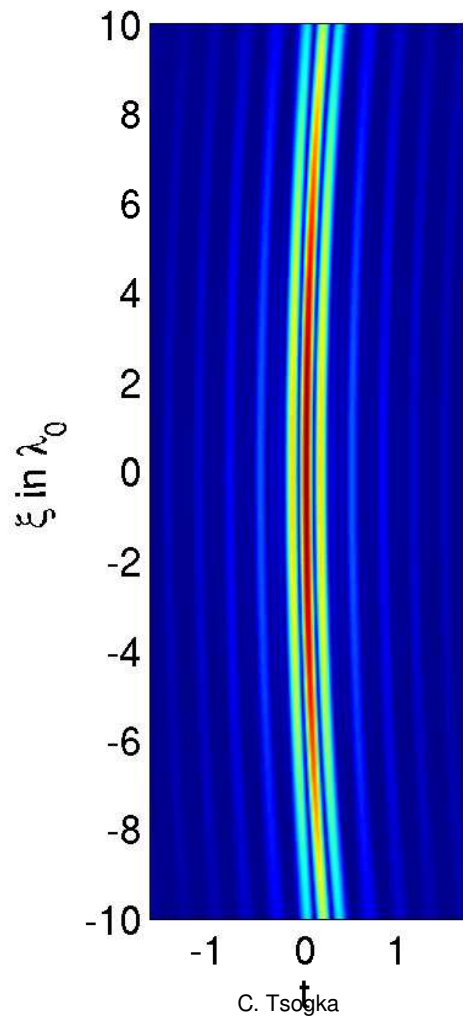
$$a_e = 9.22\lambda_0, 10.49\lambda_0 \text{ and } 9.26\lambda_0.$$

- The theoretical plot for  $\Gamma_R^{\text{TR}}(\xi, L; t)$  is obtained using  $a_e = 10\lambda_0$ .

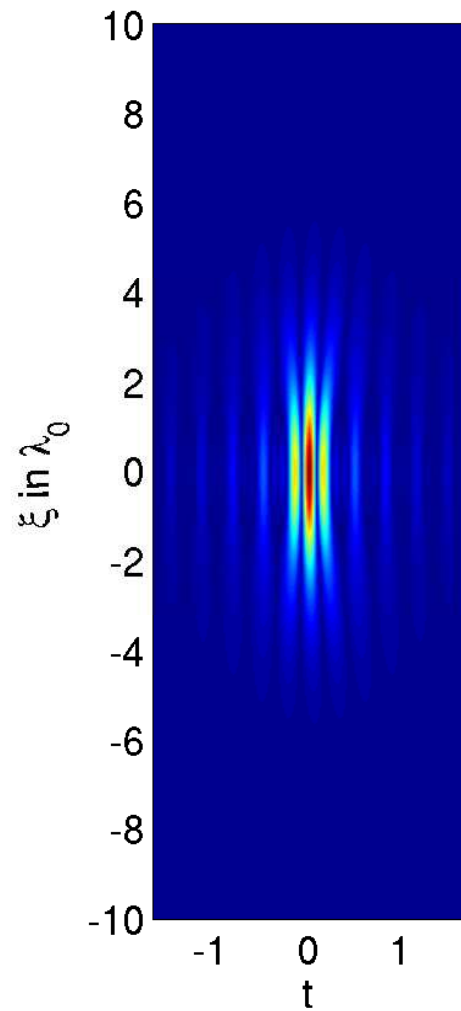
# TR focusing random media

$$\Gamma_R^{\text{TR}}(\xi, L; t), t \times \xi : [-2, 2] \text{ms} \times \xi \in [-10, 10] \lambda_0$$

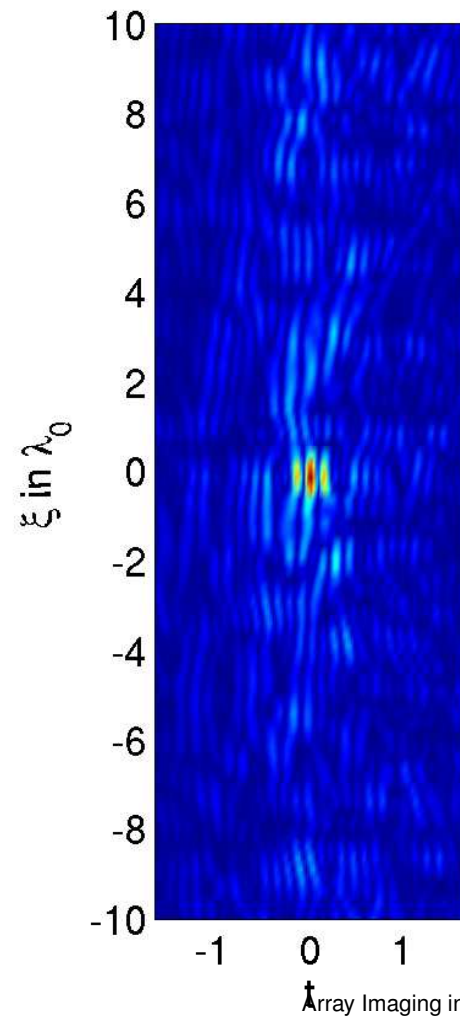
Homogeneous



Random: Theory



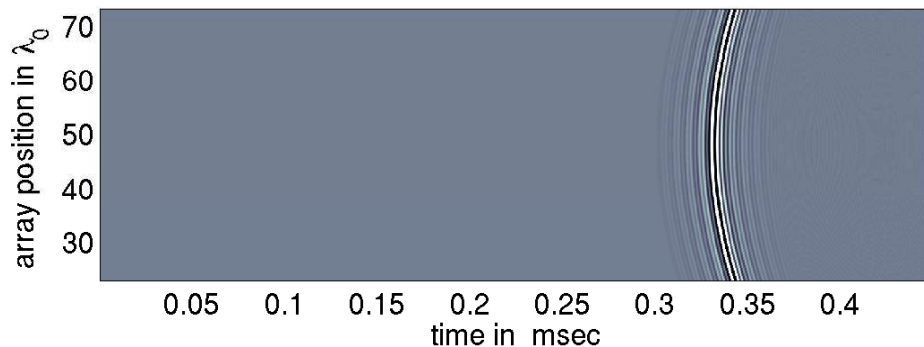
Numerics



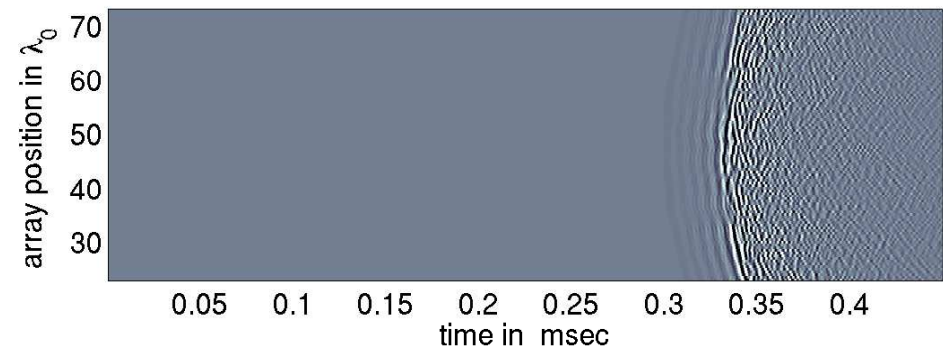
# $a_e$ estimation using CINT

- We consider here the same numerical setup with a bigger array composed by 101 elements, which means that  $a = 50\text{cm}$ .

Homogeneous



Clutter



# $a_e$ estimation using CINT

---

- We consider here the same numerical setup with a bigger array composed by 101 elements, which means that  $a = 50\text{cm}$ .
- Using the adaptive CINT we find the decoherence parameters  $\Omega_d$  and  $\kappa_d$ . From  $\kappa_d$  we can get another estimate for  $a_e$  as,

$$a_e = L\kappa_d = \frac{c_0 L}{\omega X_d(\omega)}$$

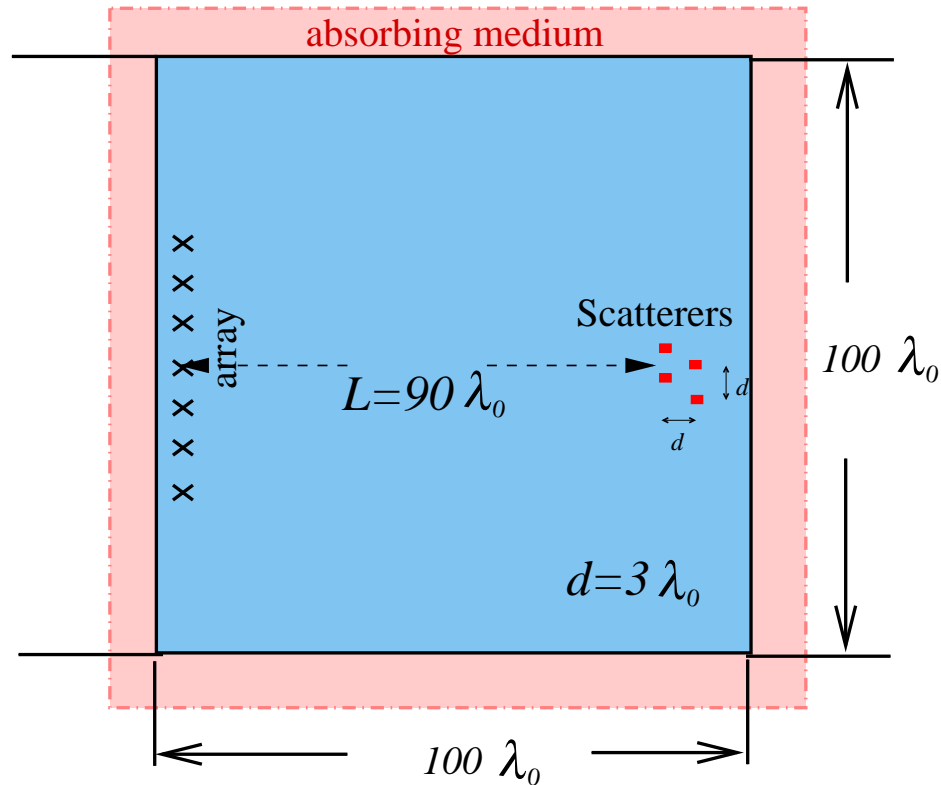
- For the same three realizations of the random medium we obtain the following estimates.

$$a_e = 9.33\lambda_0, 10.93\lambda_0, \text{ and } 11.47\lambda_0.$$

---

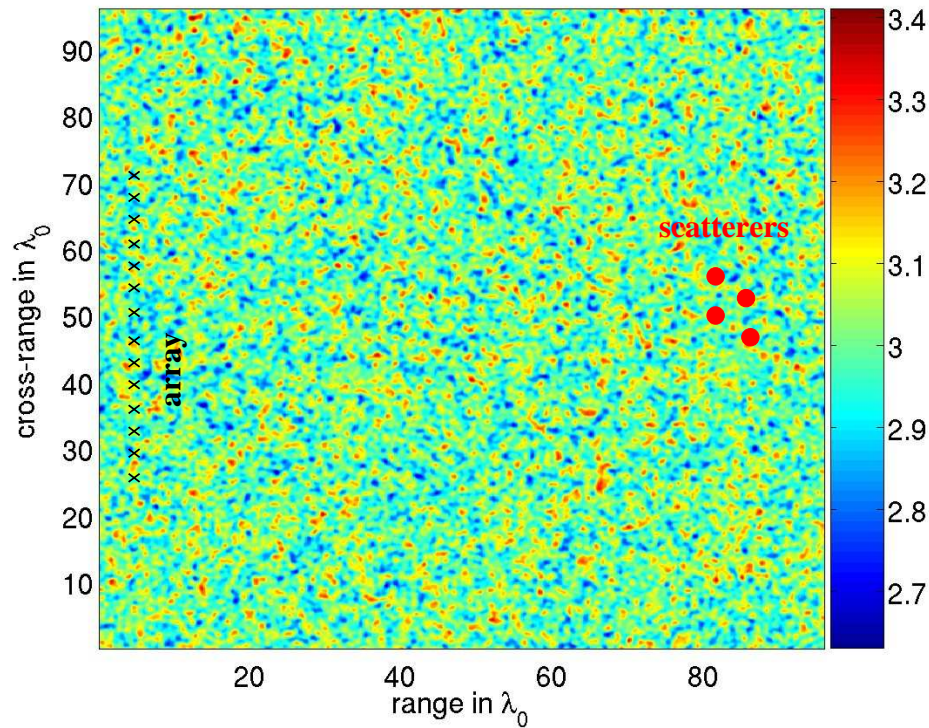
# More challenging examples

# Not well separated objects



- frequency range 150 – 450KHz,  $c_0 = 3\text{Km/s}$ ,  $\lambda_0 = 1\text{cm}$
- linear array with  $N = 100$  elements of aperture  $a = 49.5\lambda_0$

# Not well separated objects

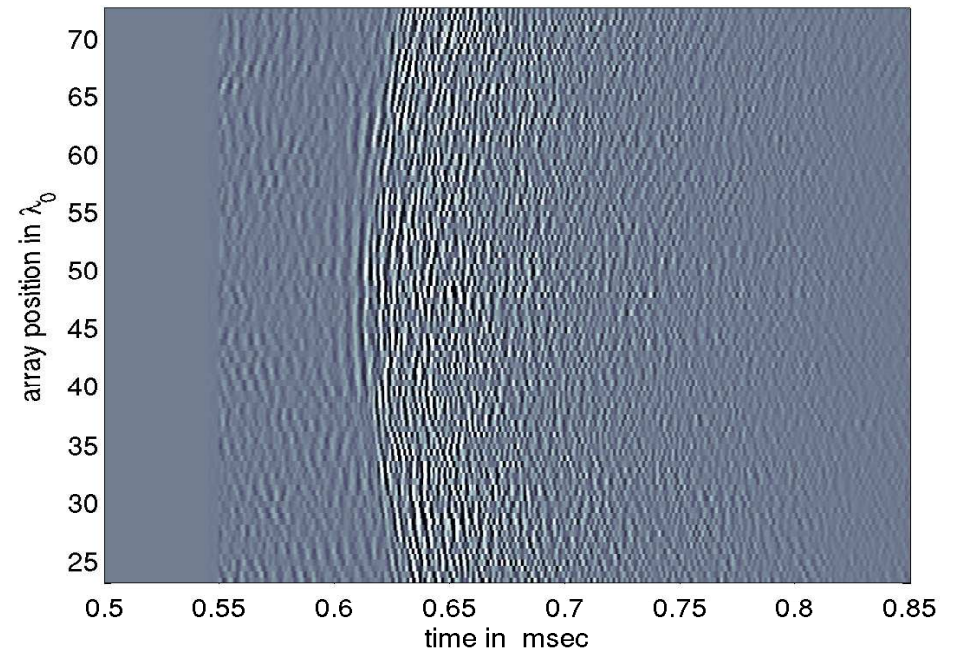
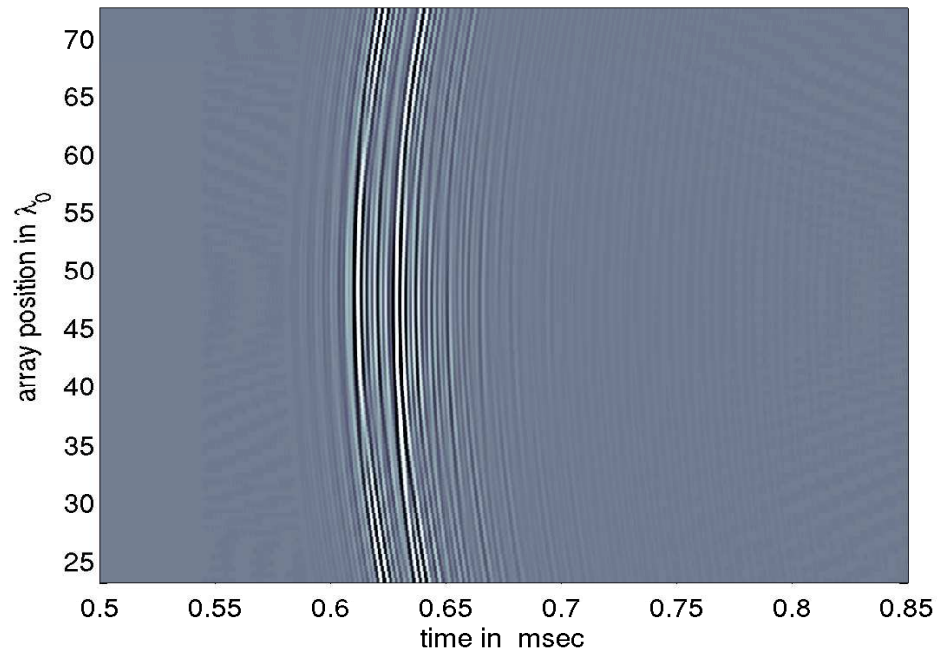


- frequency range 150 – 450KHz,  $c_0 = 3\text{Km/s}$ ,  $\lambda_0 = 1\text{cm}$
- linear array with  $N = 100$  elements of aperture  $a = 49.5\lambda_0$
- $\ell = 0.5\lambda_0$ ,  $\sigma = 0.03$  and Gaussian correlation function:

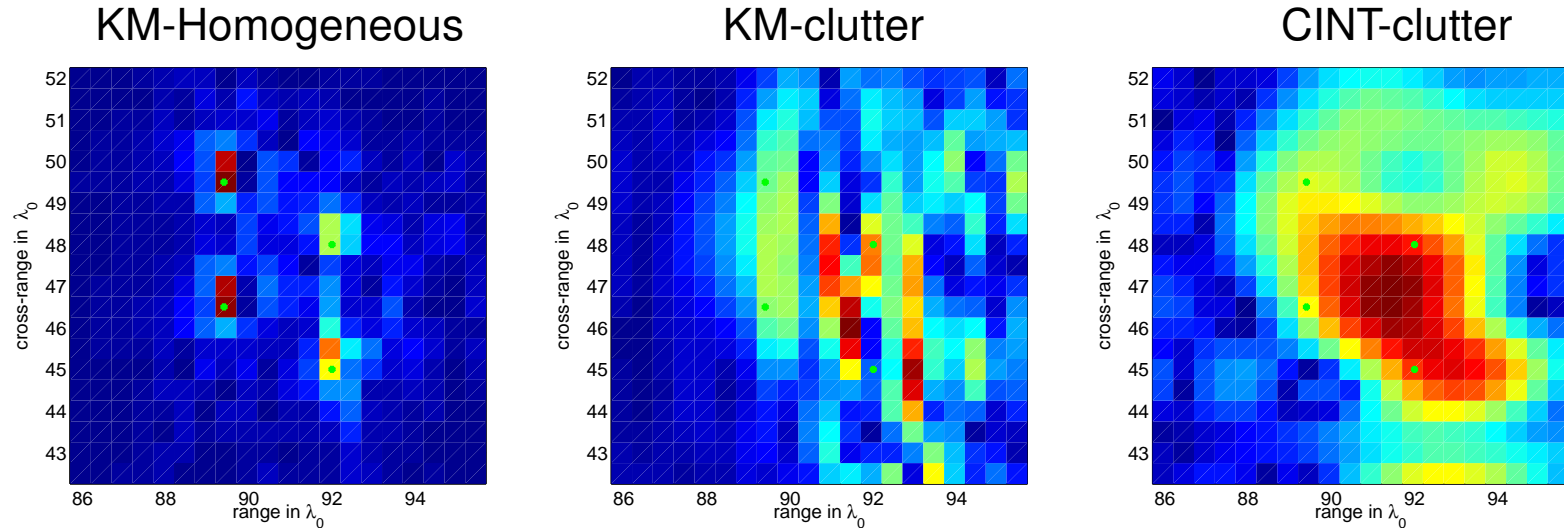
$$R(\mathbf{x}, \mathbf{x}') = R(|\mathbf{x} - \mathbf{x}'|) = e^{-\frac{|\mathbf{x} - \mathbf{x}'|^2}{2\ell^2}}$$

# Data on the array: traces

---

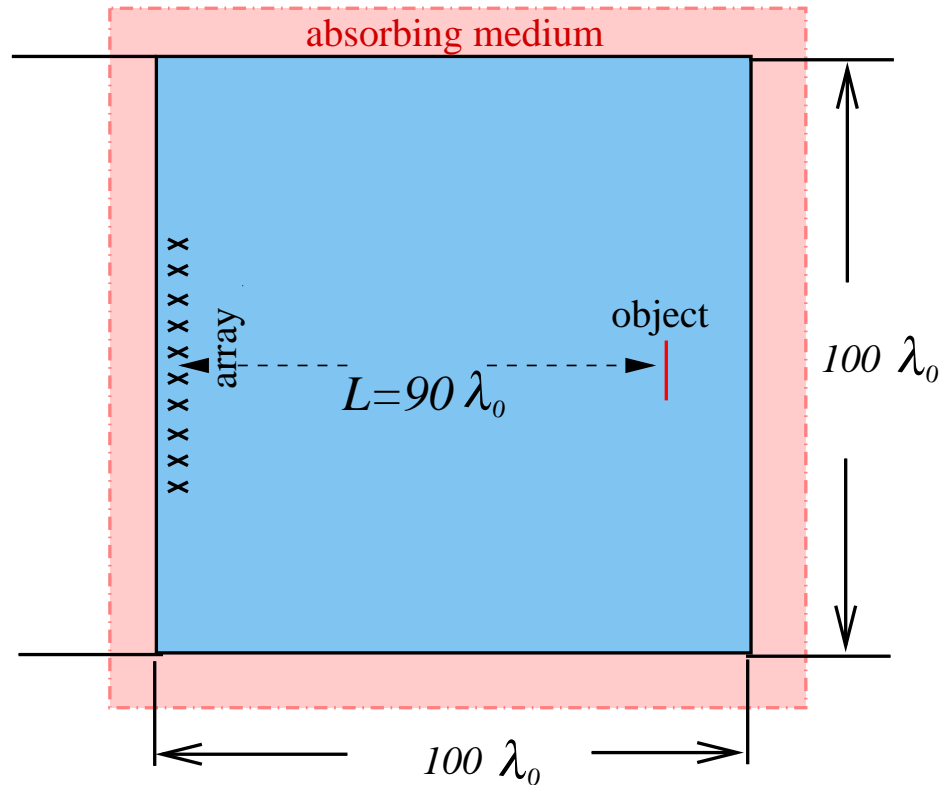


# Imaging results



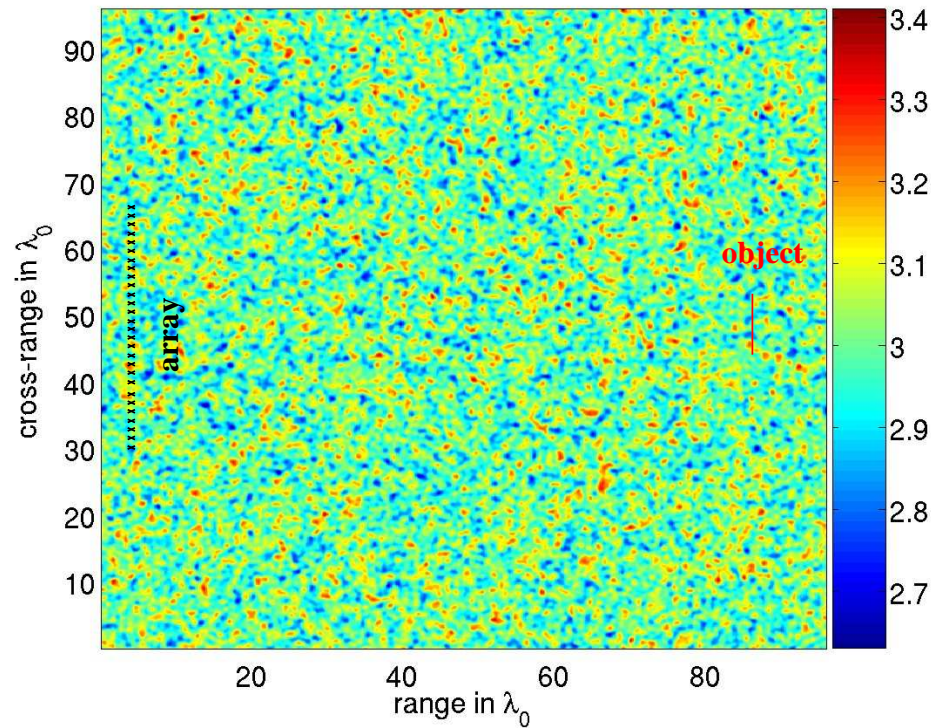
There is not enough resolution to distinguish the scatterers  $\Rightarrow$  we need selectivity (SVD)

# A crack



- Frequency range 150 – 450KHz,  $c_0 = 3\text{Km/s}$ ,  $\lambda_0 = 1\text{cm}$ .
- Linear array with  $N = 100$  elements of aperture  $a = 49.5\lambda_0$ . The range is  $L = 90\lambda_0$ . Object size is  $b = 12\lambda_0$  (Dirichlet).

# A crack



For the clutter:

- $\mu$  has a Gaussian correlation function

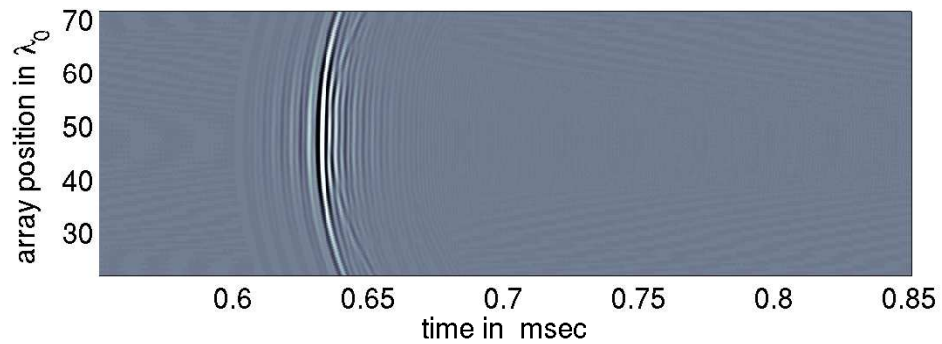
$$R(\mathbf{x}, \mathbf{x}') = \langle \mu(\mathbf{x})\mu(\mathbf{x}') \rangle = R(|\mathbf{x} - \mathbf{x}'|) = e^{-\frac{|\mathbf{x} - \mathbf{x}'|^2}{2\ell^2}}$$

- with  $\ell = 0.5\lambda_0$  and  $\sigma = 0.03$

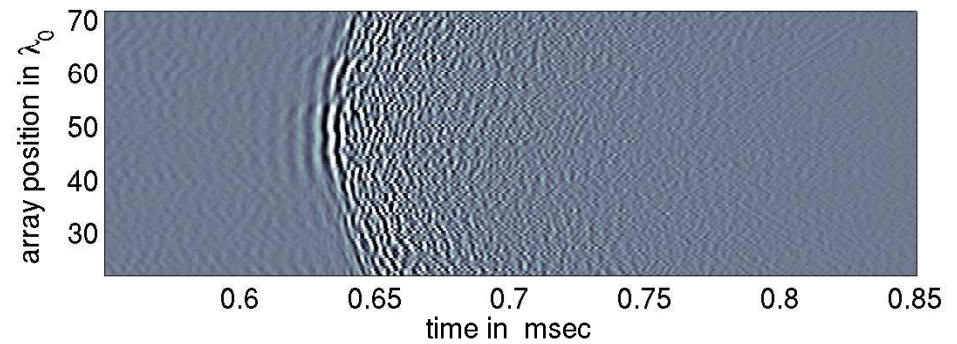
# Data on the array: traces

---

Homogeneous

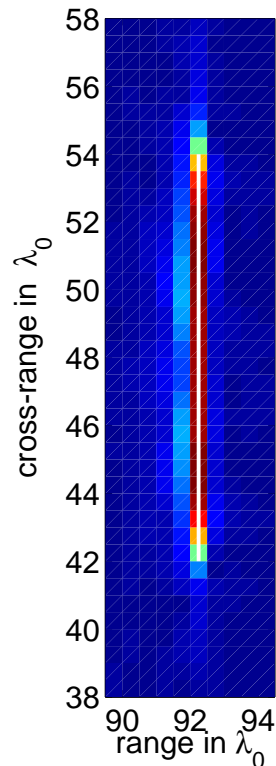


Clutter

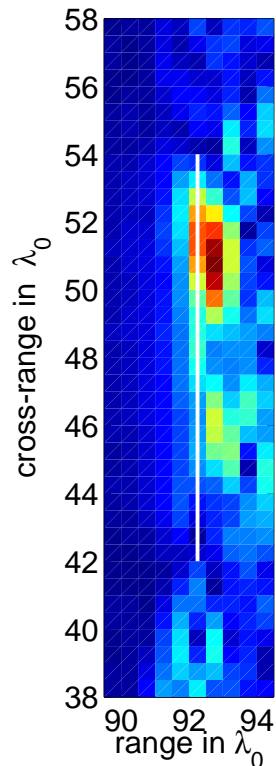


# Imaging results

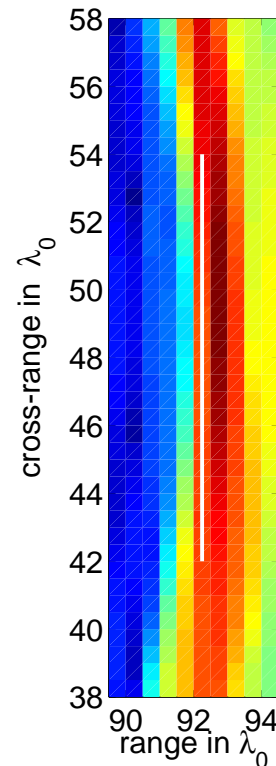
KM-Homogeneous



KM-clutter



CINT-clutter



Not enough resolution to obtain a good estimate of the size of the scatterer  $\Rightarrow$  we need selectivity that we obtain using the SVD of the response matrix (full matrix is needed).

# SVD of the response matrix

---

- The singular value decomposition of  $\Pi(\omega)$  is

$$\hat{\Pi}(\omega) = \sum_{j=1}^N \sigma_j(\omega) \hat{\mathbf{u}}_j(\omega) \hat{\mathbf{v}}_j^*(\omega),$$

\* denotes complex conjugate and transpose.

- $\sigma_j(\omega) \geq 0$  are the singular values and  $\hat{\mathbf{u}}_j(\omega)$ ,  $\hat{\mathbf{v}}_j(\omega)$  are the orthonormal left and right singular vectors.

Because  $\hat{\Pi}(\omega)$  is symmetric, we have  $\hat{\mathbf{u}}_j(\omega) = \hat{\mathbf{v}}_j^*(\omega)$ .

# Data filtering

- We define the filtered data

$$\begin{aligned} D(\omega, d)\hat{\Pi}(\omega) &= \sum_{j=1}^N d_j(\omega)\mathcal{P}_j(\omega)\hat{\Pi}(\omega) \\ &= \sum_{j=1}^N d_j(\omega)\sigma_j(\omega)\hat{\mathbf{u}}_j(\omega)\hat{\mathbf{v}}_j^*(\omega), \end{aligned}$$

- where  $\mathcal{P}_j(\omega) = \hat{\mathbf{u}}_j(\omega)\hat{\mathbf{u}}_j^*(\omega)$  is the projection matrix onto the space spanned by the  $j$ -th left singular vector.
- the coefficient  $d_j(\omega)$  is given by

$$d_j(\omega) = \begin{cases} 1 & \text{if } j \in J(\omega) \\ 0 & \text{otherwise.} \end{cases}$$

# Data filtering

- We define the filtered data

$$\begin{aligned} D(\omega, d)\hat{\Pi}(\omega) &= \sum_{j=1}^N d_j(\omega)\mathcal{P}_j(\omega)\hat{\Pi}(\omega) \\ &= \sum_{j=1}^N d_j(\omega)\sigma_j(\omega)\hat{\mathbf{u}}_j(\omega)\hat{\mathbf{v}}_j^*(\omega), \end{aligned}$$

- $J(\omega)$  determines which singular vectors we keep:
  - For  $J(\omega) = \{1, \dots, N\}$ , we keep all the singular vectors and the filter becomes the identity.
  - For  $J(\omega) = \{1\}$ , we only keep the singular vector that corresponds to the 1-st singular value. This is similar to the DORT method by Prada et al.

# Choosing the set $J(\omega)$

- $J(\omega) = 1$  is good for detection not for imaging.
- $J(\omega)$  can be chosen via an optimization approach based on the quality of the image. This is feasible when the number of significant singular values is small

(L. Borcea, G. Papanicolaou, CT, *Optimal illumination and waveform design for imaging in random media*, J. Acoust. Soc. Am., 2007).

- $J(\omega)$  can be chosen so that the normalized singular values  $\sigma_j(\omega)/\sigma_1(\omega)$  of  $\hat{\Pi}(\omega)$  belong to some interval  $[a, b]$  with  $0 < a < b < 1$ ,

$$J(\omega; [a, b]) = \left\{ j \mid \frac{\sigma_j(\omega)}{\sigma_1(\omega)} \in [a, b] \right\}.$$

# Selected subspace migration

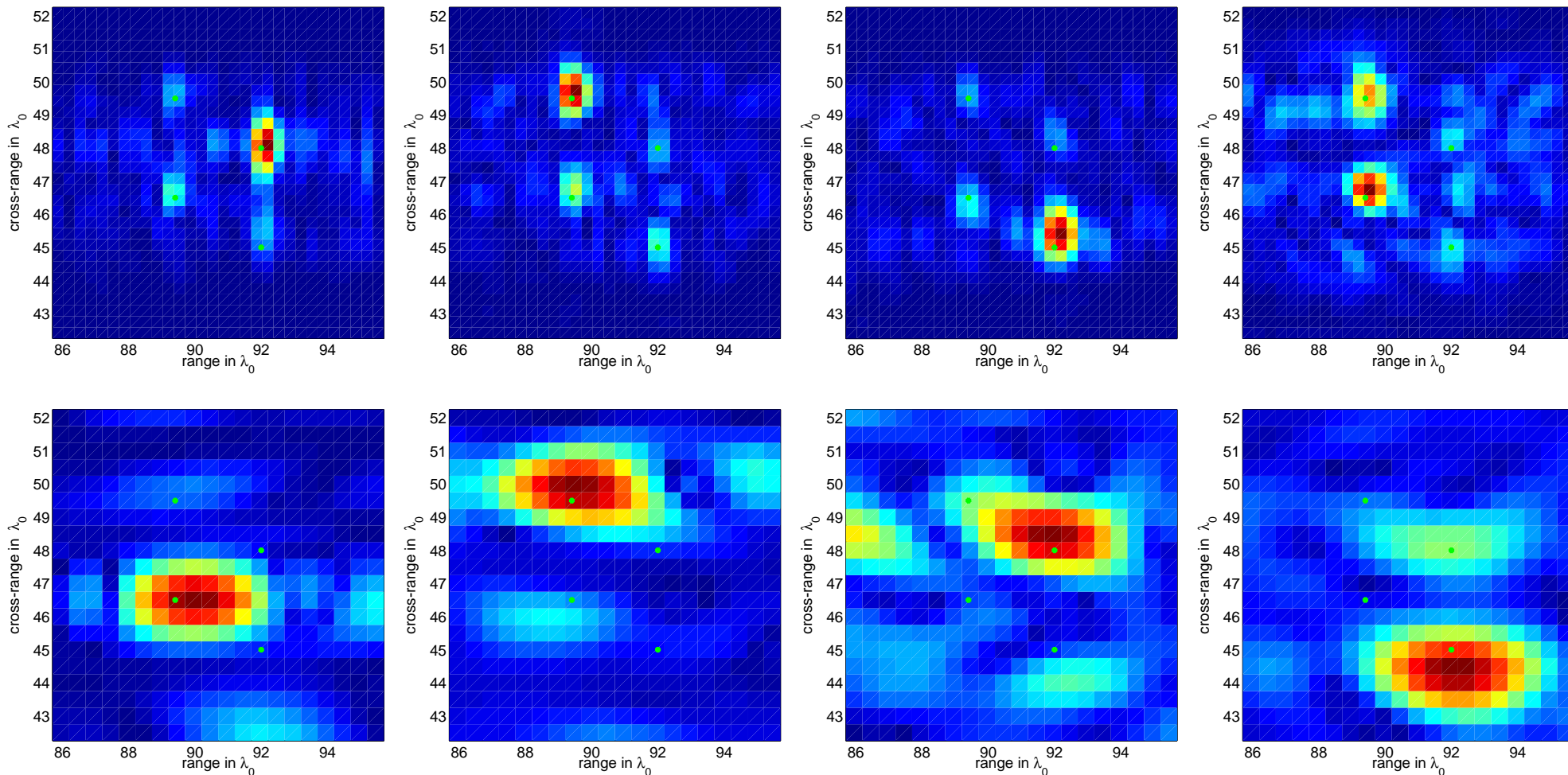
---

- For points  $\mathbf{y}^s$  in the search domain, we compute

$$\mathcal{I}^{\text{SM}}(\mathbf{y}^s) = \sum_{r=1}^{N_r} \sum_{s=1}^{N_r} \int d\omega [D(\omega, d) \hat{\Pi}(\omega)]_{r,s} \overline{G_0(\mathbf{x}_s, \mathbf{y}^s, \omega) G_0(\mathbf{x}_r, \mathbf{y}^s, \omega)}$$

- we replace  $\hat{\Pi}(\omega)$  by  $D(\omega, d) \hat{\Pi}(\omega)$  and sum over sources and receivers.
- The same can be done with CINT, we call the resulting functional SCINT.

# Four scatterers: imaging results



● top row: homogeneous, bottom row: cluttered

●  $J(\omega)$  is chosen with optimization

# A few words on the theory (crack)

---

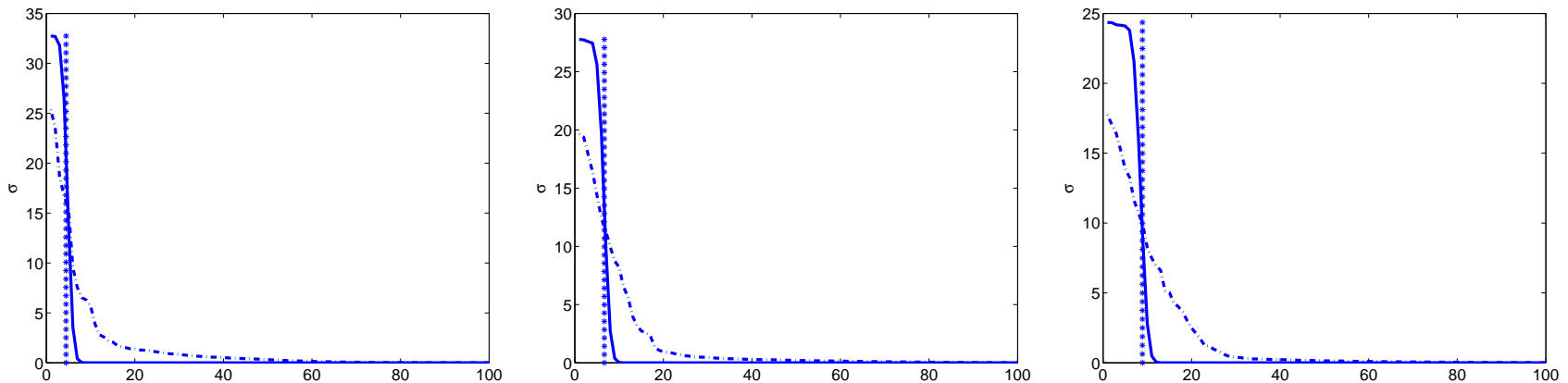
- The number of significant singular values of  $\hat{\Pi}(\omega)$  is  $N(\omega) \approx b/(\lambda L/a)$ : the number of focal spots that fit in the object.
- The significant singular values are close to a constant value and then they plunge quickly to zero.
- The singular vectors corresponding to singular values in the plunge region contain information about the boundary of the object. Information about the boundary is redundant in the plunge region.

# A few words on the theory (crack)

---

- The analysis uses properties of space and wavenumber limited functions. In the case of the crack the singular functions are the prolate spheroidal wavefunctions and they can be computed analytically.
- For cracks the analysis is done in L. Borcea, G. Papanicolaou and CT, *Optimal waveform design for array imaging*, Inverse Problems, 2007.
- For more general objects in L. Borcea, G. Papanicolaou and F. Guevara Vasquez, *Edge illumination and imaging of extended reflectors*, SIAM Journal on Imaging Sciences, 2008.

# The singular values of $\hat{\Pi}(\omega)$



The singular values of  $\hat{\Pi}(\omega)$  for the homogeneous (continuous line) and the cluttered (.- line) medium for frequencies 200kHz (left), 300kHz (middle) and 400kHz (right). The vertical line is the theoretical transition value  $N(\omega) = b/(\lambda L/a)$  which is approximately 5, 7 and 9 respectively.

# Imaging results

---

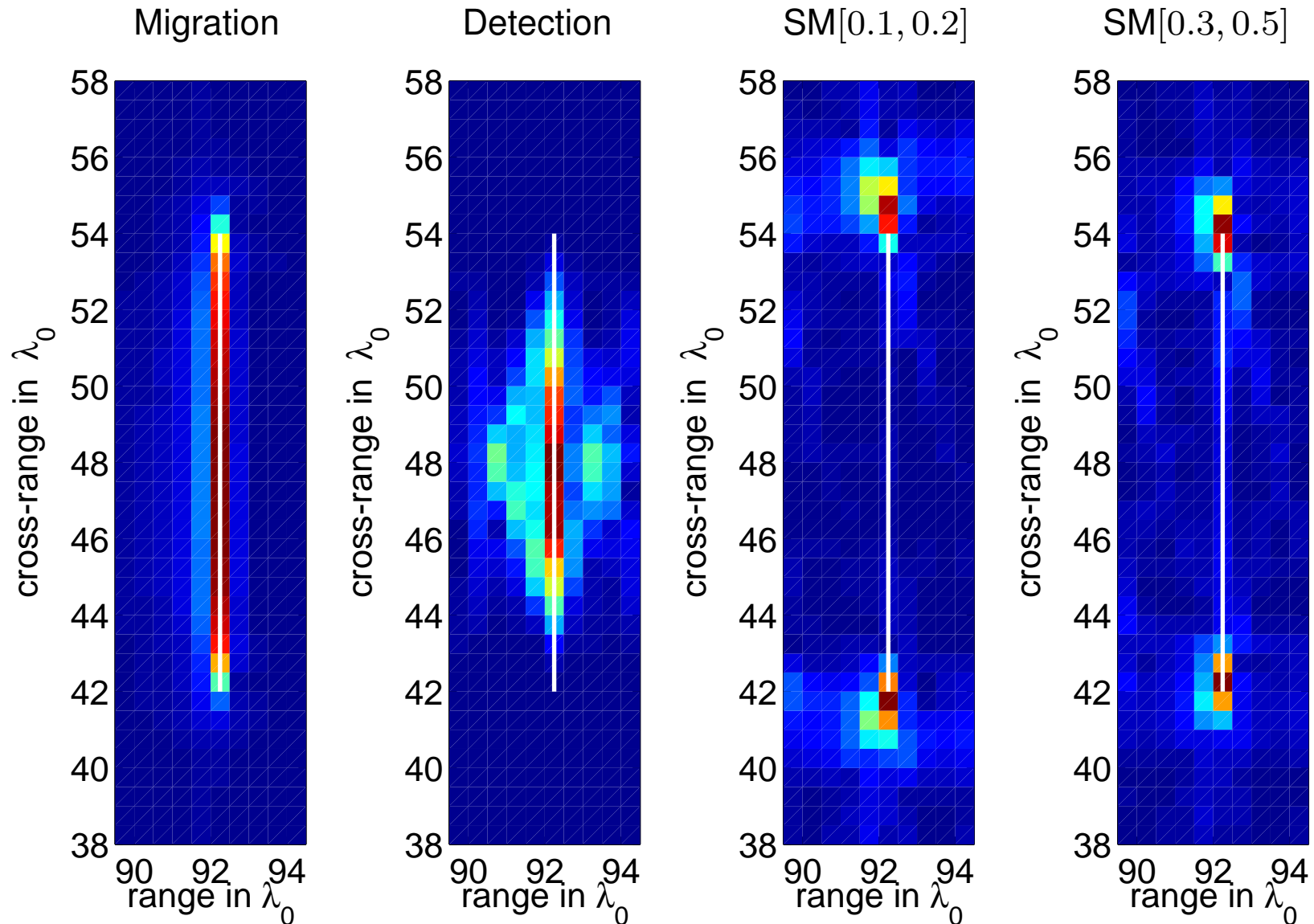
- The results are displayed in a rectangular domain of size  $5\lambda_0 \times 20\lambda_0$ . The pixel size is  $\lambda_0/2 \times \lambda_0/2$ .
- The decoherence parameters are  $\kappa_d = 0.12$  and  $\Omega_d = B/3 = 100\text{Hz}$ .

- The notation  $SM[a, b]$  (or  $SCINT[a, b]$ ) indicates that selected subspace migration (or CINT) is used with

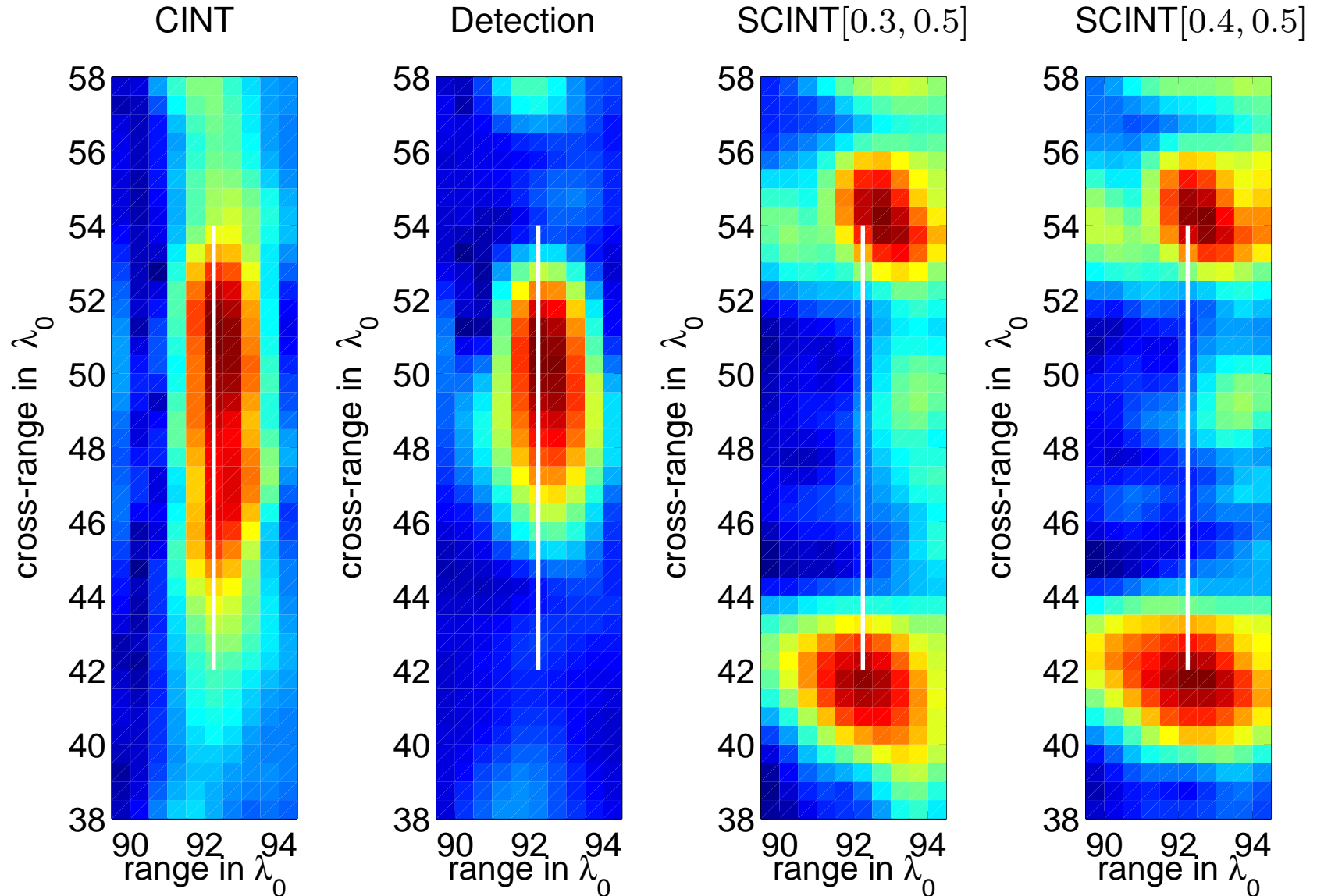
$$J(\omega; [a, b]) = \left\{ j \left| \frac{\sigma_j(\omega)}{\sigma_1(\omega)} \in [a, b] \right. \right\}.$$

- Detection means that only the first singular vector is used,  $J(\omega) = \{1\}$ .

# Imaging results - Homogeneous



# Imaging results - Clutter



# Some challenges

---

- generate realistic data (3D)!
- develop faster (smarter) algorithms for solving the wave equation (not resolving all the scales)
- optimization algorithms (big number of unknowns)
- apply imaging methodologies to real data (seismic, sonar) ...
- generalize methods to other type of waves (elastic, electromagnetic).